Journal of Inflammation Research

Dovepress
open access to scientific and medical research

Open Access Full Text Article

ORIGINAL RESEARCH

Omarigliptin Protects the Integrity of the Blood–Brain Barrier After Intracerebral Hemorrhage in Mice

Yan Zhang[1,2], Yang Liu[1,2], Xiangyu Zhang[1,2], V Wee Yong[3], Mengzhou Xue[1,2]

[1]Department of Cerebrovascular Diseases, The Second Affiliated Hospital of Zhengzhou University, Zhengzhou, Henan, People's Republic of China; [2]Academy of Medical Science, Zhengzhou University, Zhengzhou, Henan, People's Republic of China; [3]Department of Clinical Neurosciences, University of Calgary, Calgary, Alberta, Canada

Correspondence: V Wee Yong, Hotchkiss Brain Institute and Department of Clinical Neurosciences, University of Calgary, Calgary, Alberta, Canada, Email vyong@ucalgary.ca; Mengzhou Xue, Department of Cerebrovascular Diseases, The Second Affiliated Hospital of Zhengzhou University, Zhengzhou, Henan, 450001, People's Republic of China, Email xuemengzhou@zzu.edu.cn

Purpose: Intracerebral hemorrhage (ICH) is a fatal disease without effective treatment. The damage of the blood–brain barrier (BBB) is a key cause of brain edema and herniation after ICH. Omarigliptin (also known as MK3102) is a potent antidiabetic that inhibits dipeptidyl peptidase (DPP4); the latter has the ability to bind and degrade matrix metalloproteinases (MMPs). The present study aims to investigate the protective effects of omarigliptin against the destruction of BBB following ICH in mice.

Methods and Materials: Collagenase VII was used to induce ICH in C57BL/6 mice. MK3102 (7 mg/kg/day) was administered after ICH. The modified neurological severity scores (mNSS) were carried out to assess neurological functions. Nissl staining was applied to evaluate neuronal loss. Brain water content, Evans blue extravasation, Western blots, immunohistochemistry and immunofluorescence were used to study the protective effects of BBB with MK3102 at 3 days after ICH.

Results: MK3102 reduced DPP4 expression and decreased hematoma formation and neurobehavioral deficits of ICH mice. This was correspondent with lowered activation of microglia/macrophages and infiltration of neutrophils after ICH. Importantly, MK3102 protected the integrity of the BBB after ICH, associated with decreased expression of MMP-9, and preservation of the tight junction proteins ZO-1 and Occludin on endothelial cells through putative degradation of MMP-9, and inhibition of the expression of CX43 on astrocytes.

Conclusion: Omarigliptin protects the integrity of the BBB in mice after ICH injury.

Keywords: intracerebral hemorrhage, dipeptidyl peptidase, blood–brain barrier, omarigliptin

Introduction

Intracerebral hemorrhage (ICH) is an intractable health burden with 17.9 million sufferers globally.[1] Although great progress has been gained due to the development of surgery for hematoma evacuation in recent years, the prognosis of ICH is far from satisfactory. The mortality rate of ICH remains as high as 68%.[1] Perihematomal edema caused by the disruption of the blood–brain barrier (BBB) is closely associated with poor outcomes after ICH.[2–5] With every milliliter increase in brain edema, the chances of malfunctioning doubles, especially for the occurrence of herniation.[6]

The BBB is mainly composed of the extracellular matrix (ECM), endothelial cells, astrocytes, and the cellular junctions (tight junction, eg, zonula occludens, ZOs; gap junction, eg, connexins, CXs; and adherence junction) between them.[7] Preclinical evidence has informed that the BBB in ICH is damaged due to the reduction of those cellular junctions (collagenase IV/VII and autologous blood injection).[8] In addition, matrix metalloproteinases (MMPs), a family of zinc-dependent endopeptidases that proteolyze ECM members, are significantly increased after ICH and cause BBB breakdown by directly degrading junctional proteins.[7,9] Therefore, targeted maintenance of BBB integrity to reduce brain edema and secondary brain injury has been an appealing therapeutic strategy for the treatment of ICH.[10]

Received: 3 March 2023
Accepted: 10 June 2023
Published: 15 June 2023

Dipeptidyl peptidase 4 (DPP4) is a membrane-associated peptidase encoded by mitochondria and widely distributed in body organs to exert pleiotropic effects via degrading target peptide, such as glucagon-like peptide-1 (GLP-1), GIP, and neuropeptide Y.[11] Recent evidence suggests that DPP4 has the ability to degrade ECM by binding to ECM directly or binding to adenosine deaminase and activating MMPs.[12] Among all MMPs, the activity of MMP9 and MMP1 was most affected by DPP4.[13] Moreover, DPP4 also mediates MMP activation and Cx43 internalization by stimulating the mitogen-activated protein kinase (MAPK) pathway.[14,15] In addition, MMPs expression and ECM degradation can be regulated by GLP-1.[16] These collective evidence suggest that DPP4 may be a potential target for protecting the BBB after ICH.

Omarigliptin (MK3102) is a novel, long-acting and potent DPP4 inhibitor for the treatment of type 2 diabetes mellitus.[17] It can cross the BBB due to its low molecular weight and lipophilic properties.[18] A recent study showed that MK3102 protected the BBB integrity destroyed by LPS stimulation.[18] However, whether the disrupted BBB would be alleviated by MK3102 after ICH injury remains unclear. In this study, we explored the potential protective effect of MK3102 on BBB after ICH in mice.

Materials and Methods

Experimental Animals

According to the number of animals, we have used in previous studies[19] and the guidelines for the design and statistical analysis of experiments using laboratory animals,[20] a minimum of 114 adult male C57BL/6 mice, weighing 20–25 g, were used in this study for achieving the scientific objectives. All mice were purchased from Beijing Vital River Experimental Animals Centre (Beijing, China) and maintained under pathogen-free conditions in a Specified Pathogen-Free room with temperature at 22°C, relative humidity at 55%, and light/dark cycle at 12/12 hours. All experimental procedures were approved by the Ethics Committee of Zhengzhou University, according to the Laboratory Animal—Guideline for Ethical Review of Animal Welfare.

The ICH Models and MK3102 Administration

Mice were anesthetized with an isoflurane-oxygen mixture during the surgical procedure and fixed to the brain stereotactic apparatus (RWD, Shenzhen, China). 0.075 U of collagenase type VII (Sigma-Aldrich, Milwaukee, WI, USA) was dissolved in 0.75 μL of saline and injected into the right mouse brain with a rate of 0.1 μL/minute, according to coordinates (located in the right basal ganglia, 2.0 mm away from the midline, 3.5 mm under the skull, and 0.2 mm posterior of the bregma). After the injection, the needle was maintained for 10 minutes to prevent reflux, and the micro-syringe needle was slowly withdrawn. Finally, bone wax was used to seal the burr hole, followed by wound suturing and disinfection. The animals were placed in a cage with ad libitum access to food and water.

All mice were randomly assigned to three groups: sham group, ICH + DMSO treated group, and ICH + MK3102 (in DMSO) treated group. Mice in the ICH group received 0.75 μL of 0.075 U collagenase type VII in the right basal ganglia, while mice in the sham group received 0.75 μL of sterile saline. For the MK3102 treatment, the MK3102 (Glpbio, USA) was dissolved in 10% DMSO and was given (7 mg/kg/day) via gavage starting from 1 hour after collagenase injection. The dosage of MK3102 was determined by the conversion of rat doses to mouse equivalent doses based on body surface area and the 11~22-hour half-life pharmacokinetic characteristics of MK3102.[18,21] Mice in the vehicle group were administered with the same volume of DMSO. All treatments were conducted for 3 days as our previous work demonstrated that the prominent pathological insult of experimental ICH was observed at 3 days after collagenase type VII injection.[9,22,23]

Hematoma Volume Measurement

Mice were anesthetized using isoflurane-oxygen mixture. After cardiac perfusion with 4% paraformaldehyde, brains were immediately removed and fixed in the same fixative fluid for 3 days. Fixed brains were cut into coronal sections of 1 mm thickness through the needle entry site. The continuous slices were digitally photographed, and the size of the hematoma

was measured by image analyzer program (Image Pro-Plus 6.0). The total hematoma volume was calculated by adding the hematoma areas in each section and multiplying by the section thickness.[11]

Nissl Staining

Nissl staining was used to evaluate the viable neurons in brain tissue. The sections embedded in paraffin were placed in the Nissl solution (Beyotime, Nanjing, China) for 10 minutes after completely dewaxing and rehydration with gradient alcohol. Pictures of Nissl stained sections were taken with Olympus microscope (Olympus Co., Japan) by using 40X objective. The viable neurons which were defined by the presence of pale nuclei and large cellular bodies were analyzed with Image Pro-Plus 6.0 software, and the sum of four fields from three sections per mouse were counted manually with Image Pro-Plus 6.0 software. Neurons with dark staining and shrunken cellular bodies were considered dead and were not included for Nissl positive cell counting.[24]

Behavioral Test

Behavioral assessment was carried out by two independent investigators blinded to the experimental groups using the modified neurological severity score (mNSS) at the 3 days after ICH. The mNSS consisted of four components: motor, sensory, reflexes absent and abnormal movements, and beam balance tests. The scores were ranged from 0 to 18. The higher scores depict a more severe brain damage according to the scoring criteria.[25]

BBB Permeability Assay

BBB permeability was evaluated with Evans blue (EB) staining as previously described with slight modifications.[26] Briefly, 250 μL of 2% EB (Sigma Aldrich, USA) solution was administered through intraperitoneal injection at 3 days following ICH. The mice were euthanized after 3 hours of EB infusion and were then perfused transcardially with saline solution. The ipsilateral/contralateral brain hemispheres were collected, weighed and homogenized in methanamide solution in a ratio of 1:10. The tissues were then placed in a water bath with a constant temperature of 60°C for 24 hours, and then centrifuged at 14,000 × g for 30 minutes. The absorbance of the supernatant was measured at 610 nm by SpectraMax M5/M5e (Molecular Devices, USA) and quantified according to a standard curve. The experimental results were expressed as the ratio of the EB content in the ipsilateral/contralateral brain.

Brain Water Content Measurement

Brain edema was assessed using the dry and wet weight method as described previously with minor modifications.[27] The brain was harvested 3 days after ICH and dissected into ipsilateral and contralateral hemisphere, and cerebellum; the latter served as an internal control. Brain tissues were weighed on an electronic analytical balance before and after drying for 72 hours at 80 °C overnight. Brain water content (%) was calculated using the following equation: $(\text{wetweight} - \text{dryweight})/\text{wetweight} \times 100\%$.

Immunohistochemistry

Brain tissues were harvested and cut into 5 μm paraffin sections on the third day after ICH. Sections from the lesion center and one each on either side spaced 200 μm from the center section were used for analysis. Briefly, sections were incubated under 4°C overnight with rabbit anti-myeloperoxidase (MPO) antibody (neutrophil marker, 1:800, Abcam, Cambridge, MA, USA) and rabbit anti-Iba1 polyclonal antibody (microglia marker, 1:400, Wako, Japan). The sections were then incubated with horseradish peroxidase-combined secondary anti-rabbit immunoglobulin G antibody (1:1000, Abcam, Cambridge, MA, USA) for 1 hour at room temperature. All staining outcomes were observed using an Olympus microscope (Olympus Co., Japan), and the positive MPO cells in 4 fields per section and 3 sections per mouse were analyzed with Image Pro-Plus 6.0 software.

For the degree of microglia/macrophage activation, the sections were analyzed blindly through determining the morphology and density of the Iba1-labeled cells as described previously.[28] Homeostatic microglia were characterized by multi-branched processes projecting from the cell soma, which retracted and thickened when microglia were activated.

Iba1-stained sections were scored for activity using a scale of 1–4, in which one represents the least reactivity and score 4 was with the highest. Considerations were applied for the size, shape, and relative density of Iba1-labeled cells.

Brain Tissue Frozen Section and Immunofluorescence Assay

Brain tissue frozen sections were prepared on the third day after ICH. Sections were incubated overnight at 4°C with rabbit anti-ZO-1 monoclonal antibody (1:100, Abcam, Cambridge, MA, USA), rabbit anti-Occludin (1:50, Affinity Biosciences, OH, USA), mouse anti-vWF (1:200, Proteintech, China), rabbit anti-CX43 (1:50, Cell Signaling, USA) and mouse anti-GFAP monoclonal antibody (1:100, Santa Cruz Biotechnology, CA, USA). The Alexa Fluor 488/594-conjugated goat anti-mouse/rabbit secondary antibody (1:500, Abbkine, California, USA) was added for 1 hour in the dark at room temperature. All sections were cover slipped using an anti-fade mounting medium with DAPI and then were observed under a fluorescent microscope (Olympus Co., Japan).

Western Blot Analysis

Mice were euthanized at 3 days after ICH, and their right brain hemisphere was extracted for Western blot analysis. The following primary antibodies were used: rabbit anti-DPP4 monoclonal antibody (1:1000, Abcam, Cambridge, MA, USA), rabbit anti-Occludin monoclonal antibody (1:1000, Abcam, Cambridge, MA, USA), rabbit anti-ZO-1 monoclonal antibody (1:5000, Proteintech, China), rabbit anti-MMP-9 monoclonal antibody (1:1000, Abcam, Cambridge, MA, USA), rabbit anti-CX43 monoclonal antibody (1:1000, Cell Signaling Technology, USA), rabbit anti-GAPDH monoclonal antibody (1:5000, Proteintech, China), and anti-α-Tubulin (1:1000, Proteintech, China). Enhanced chemiluminescence detection kit was employed to visualize immunoblots. The relative intensity of the bands was measured by ImageJ (NIH, United States).

Ethidium Bromide Staining

Ethidium bromide staining was used as a surrogate the activity of connexin 43 hemichannels.[29] The sections were placed in the 0.01% ethidium bromide solution (Selleck, USA) for 2 minutes after completely dewaxed and rehydrated with gradient alcohol. Pictures of ethidium bromide staining were taken with Olympus microscope (Olympus Co., Japan) by using 40X objective. The ethidium bromide positive cells in 4 fields per section and 3 sections per mouse were counted manually with Image Pro-Plus 6.0 software.

Statistical Analysis

Statistical analyses were performed by the GraphPad Prism Version 6.0 (GraphPad, La Jolla, CA, USA). All data obtained were presented as mean ± standard deviation (SD). The Shapiro–Wilk test and/or D'Agostino & Pearson omnibus normality test were used to evaluate data normality. Comparisons between multiple groups were made using one-way analysis of variance (ANOVA), followed by Tukey's Honestly Significant Difference (HSD) post-hoc test. The Kruskal–Wallis test was used to analyze data that did not exhibit the normal/Gaussian distribution. $P < 0.05$ was defined as statistically significant.

Results

Brain DPP4 Was Upregulated After ICH in Mice

We used Western blotting to examine the protein expression level of DPP4 after ICH. Our results showed an elevated expression of DPP4 in the ICH group compared to the sham group 3 days after ICH injury. Treatment with MK3102 after ICH markedly decreased DPP4 level compared to that in the ICH + DMSO group (0.8480 ± 0.08551 versus 1.085 ± 0.1114, $p < 0.01$, Figure 1).

Inhibition of DPP4 with MK3102 Decreased Hematoma Formation and Neurobehavioral Deficits After ICH

We determined whether DPP4 inhibition has neuroprotective effects in mice after ICH. The coronal sections of brain showed an obvious hematoma after collagenase injection (sham, 0.2606 ± 0.5193 mm^3 versus ICH + DMSO, 11.69 ± 0.2119 mm^3, $p < 0.0001$; versus ICH + MK3102, 9.915 ± 0.7199 mm^3, $p < 0.0001$, Figure 2A and B). MK3102 treatment significantly decreased hematoma volume when compared with ICH + DMSO treated group (9.915 ± 0.7199 mm^3 versus $11.69 \pm$

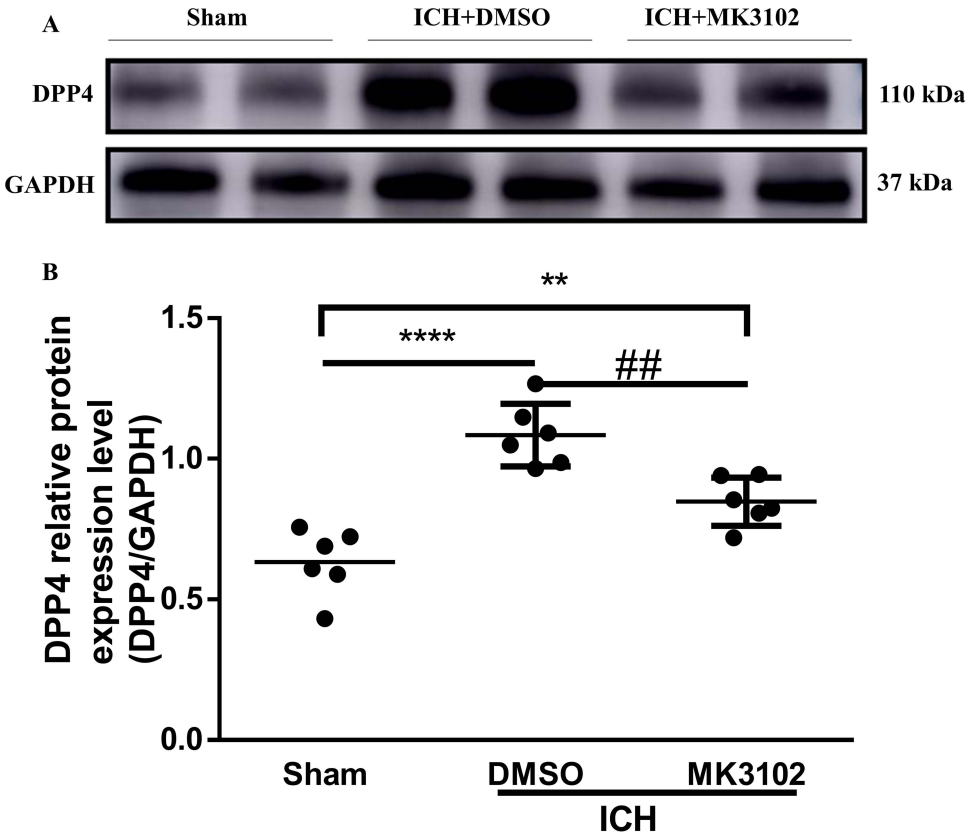

Figure 1 Brain DPP4 was upregulated after ICH in mice. (**A**) Representative Western blot bands of DPP4. (**B**) Quantitative analyses of relative protein level of DPP4 at 3 days after ICH. n = 6 per group. All data are displayed as mean ± SD. The difference between groups was analyzed using One-way ANOVA test. **p<0.01, ****p<0.0001 compared with sham group. ##p<0.01 compared with the ICH + DMSO group.

0.2119 mm^3, $p < 0.001$, Figure 2A and B) at 3 days after injury. Data obtained by Nissl staining show a smaller number of viable neurons in the area adjacent to hematoma in the ICH group compared to the sham group 3 days after ICH. MK3102 treatment markedly preserved the number of viable neurons compared with that in the ICH + DMSO group (891.4 ± 92.05 versus 540.6 ± 94.19, $p < 0.0001$, Figure 2C and D). Moreover, the mNSS highlighted a better functional outcome in ICH +MK3102 group compared with vehicle treatment group (10.10 ± 2.079 versus 13.60 ± 1.776, $p < 0.001$, Figure 2E). These results indicate that inhibition of DPP4 with MK3102 exerts a neuroprotective effect in ICH in mice.

MK3102 Protected the BBB Integrity Destroyed by ICH and Decreased Brain Edema

The EB leakage test was used to evaluate the integrity of the BBB. Our quantitative results show that ICH significantly increased EB dye leakage from vessels. Compared to vehicle, treatment with MK3102 markedly decreased the EB dye leakage compared with that in the ICH + DMSO group (1.161 ± 0.04222 versus 1.406 ± 0.05866, $p < 0.0001$, Figure 3A).

Brain edema was determined by brain water content. A significant increase of brain water content was observed in the ipsilateral hemisphere in ICH group, but no significant difference was observed in the contralateral hemisphere or cerebellum (as an internal control). MK3102 significantly decreased brain water content in the ipsilateral hemisphere compared with that in the ICH + DMSO group (78.63 ± 0.6836% versus 81.05 ± 0.7040%, $p < 0.05$, Figure 3B).

MK3102 Restrained the Activation of Microglia/Macrophages and Reduced Infiltration of Neutrophils After ICH

Our immunostaining results show that activated microglia/macrophages and infiltrated neutrophils were elevated in the ICH + DMSO group compared with the sham controls (activated microglia/macrophages: ICH + DMSO, 3.300 ± 0.4631 versus sham, 1.294 ± 0.04374, $p < 0.0001$; infiltrated neutrophils: ICH + DMSO, 650.2 ± 24.47 versus sham, 7.600 ± 10.16; $p < 0.0001$, respectively, Figure 4). MK3102 intervention significantly reduced the representation of activated

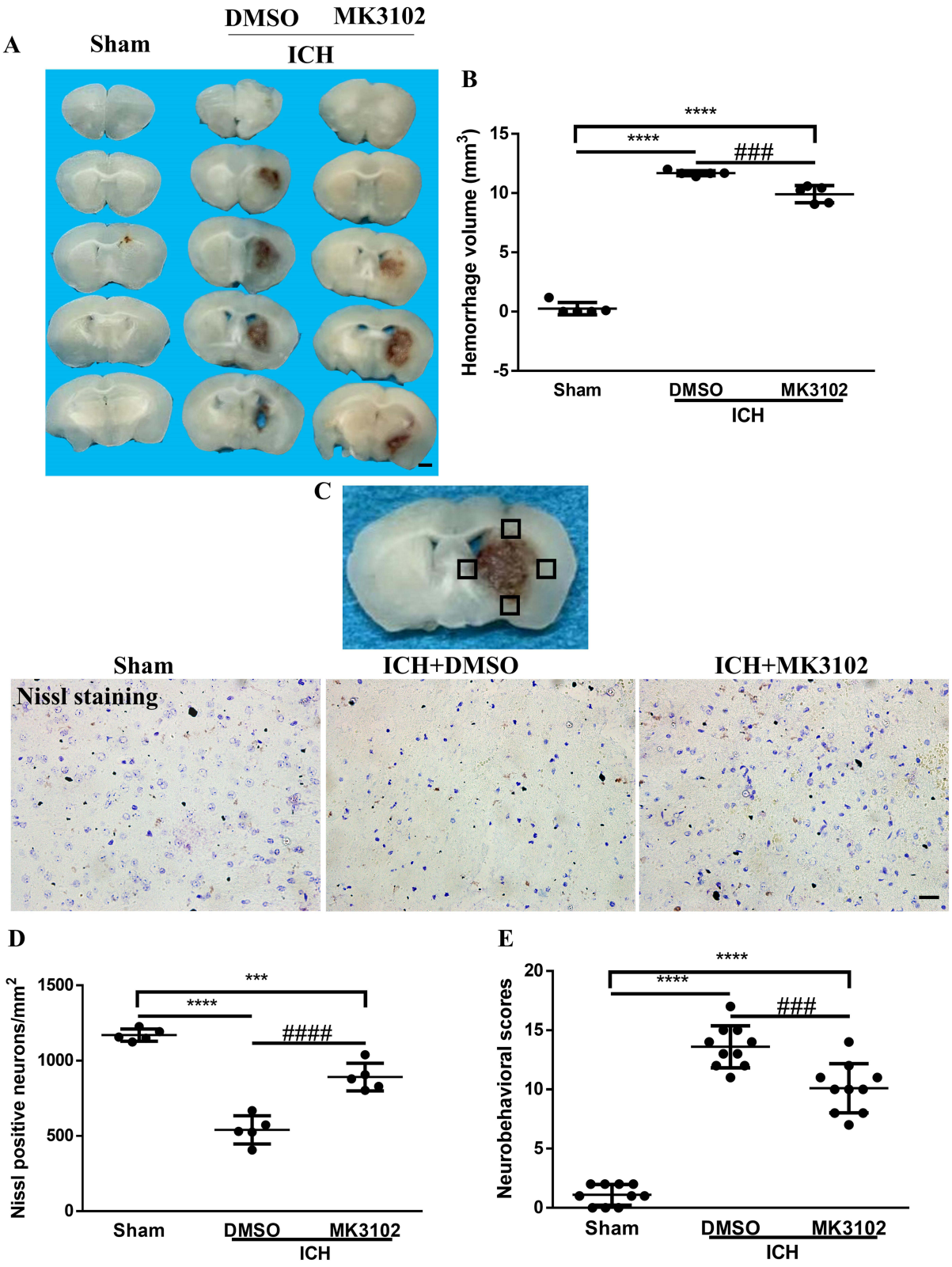

Figure 2 MK3102 reduced hematoma size and improved functional recovery after ICH. (**A**) Representative photographs of coronal sections of brain tissue at 3 days after ICH. Scale bar, 1 mm. (**B**) Quantitative analysis of hematoma volume. n = 5 per group. (**C**) Representative microphotographs of Nissl staining in the perihematomal area. Scale bar, 20 μm. The small black squares in the coronal section of brain indicate the area where microphotograph was taken. (**D**) Quantitative analysis of Nissl positive cells in the perihematomal area at 3 days after ICH. n = 5 per group. (**E**) Quantitative analysis of neurological scores at 3 days after ICH. n = 10 per group. All data are displayed as mean ± SD. The difference between groups was analyzed using One-way ANOVA test. ***p<0.001, ****p<0.0001 compared with sham group. $^{\#\#\#}$p<0.001, $^{\#\#\#\#}$p<0.0001 compared with the ICH + DMSO group.

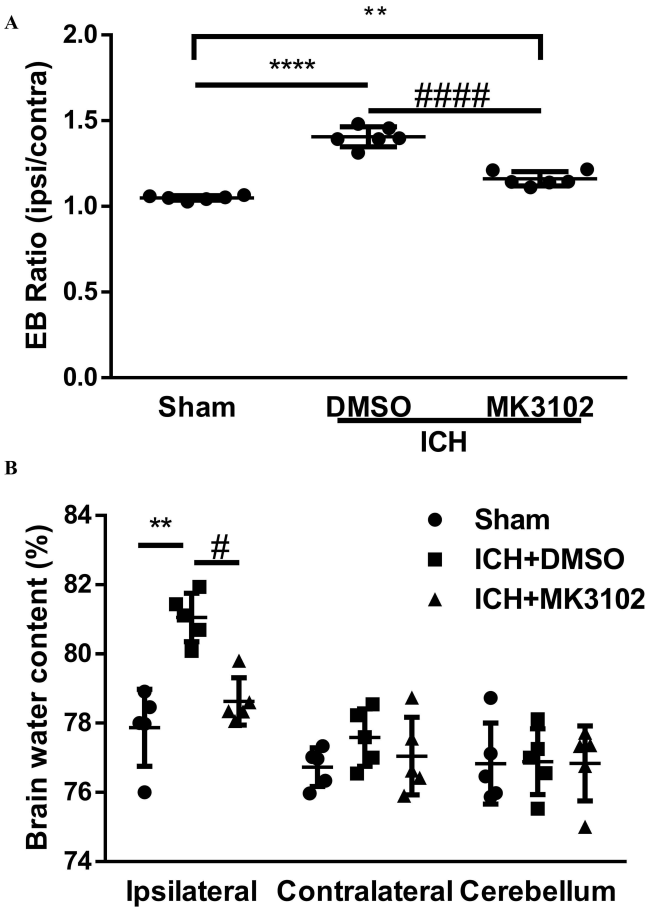

Figure 3 MK3102 decreased Evans blue extravasation and brain water content at 3 days after ICH. (**A**) Quantitative analyses of Evans blue extravasation (Ipsilateral/Contralateral). n = 6 per group. (**B**) Quantitative analyses of brain water content (%). n = 5 per group. All data are displayed as means ± SD. The difference between groups was analyzed using One-way ANOVA test. **p<0.01, ****p<0.0001 compared with sham group. #p<0.05, ####p<0.0001 compared with the ICH + DMSO group.

microglia/macrophages (2.258 ± 0.4654 versus 3.300 ± 0.4631, $p < 0.01$) and infiltrated neutrophils (544.6 ± 60.92 versus 650.2 ± 24.47; $p < 0.01$) compared to the ICH + DMSO group (Figure 4).

MK3102 Reduced MMP-9 Expression and Preserved the Tight Junction Protein ZO-1 and Occludin on Endothelial Cells After ICH Injury in Mice

Western blot results showed that the expression level of ZO-1 and Occludin was downregulated, while MMP-9 was markedly increased after ICH injury. Compared to the ICH + DMSO group, MK3102 significantly decreased the expression level of MMP-9 while increasing the level of ZO-1 and Occludin after ICH injury (MMP-9: ICH + MK3102, 0.6362 ± 0.1409 versus ICH + DMSO, 0.9338 ± 0.1338, $p < 0.05$; ZO-1: ICH + MK3102, 1.003 ± 0.09752 versus ICH + DMSO, 0.7951 ± 0.1522, $p < 0.05$; Occludin: ICH + MK3102, 1.023 ± 0.04652 versus ICH + DMSO, 0.6778 ± 0.1326, $p < 0.01$, respectively, Figure 5A–D). In addition, the immunofluorescence co-location results of ZO-1 and Occludin with vWF (endothelial cell marker) corroborated that ICH can cause endothelial cell death, as well as the degradation of ZO-1 and Occludin on endothelial cells. However, MK3102 treatment significantly promoted endothelial cell survival and inhibited the degradation of ZO-1 and Occludin on vascular endothelial cells by MMP-9, thus protecting the integrity of BBB after ICH (Figure 5E).

MK3102 Inhibited the Expression of CX43 Hemichannels on Astrocytes

Astrocytes are the main response cells to neuroinflammation in the brain after ICH, and the abnormal opening of CX43 hemichannels on astrocytes triggers the release of inflammatory mediators to destruct the BBB. Therefore, in order to evaluate the effect of MK3102 on astrocytes, we observed the expression of CX43 hemichannels on astrocytes by immunofluorescence

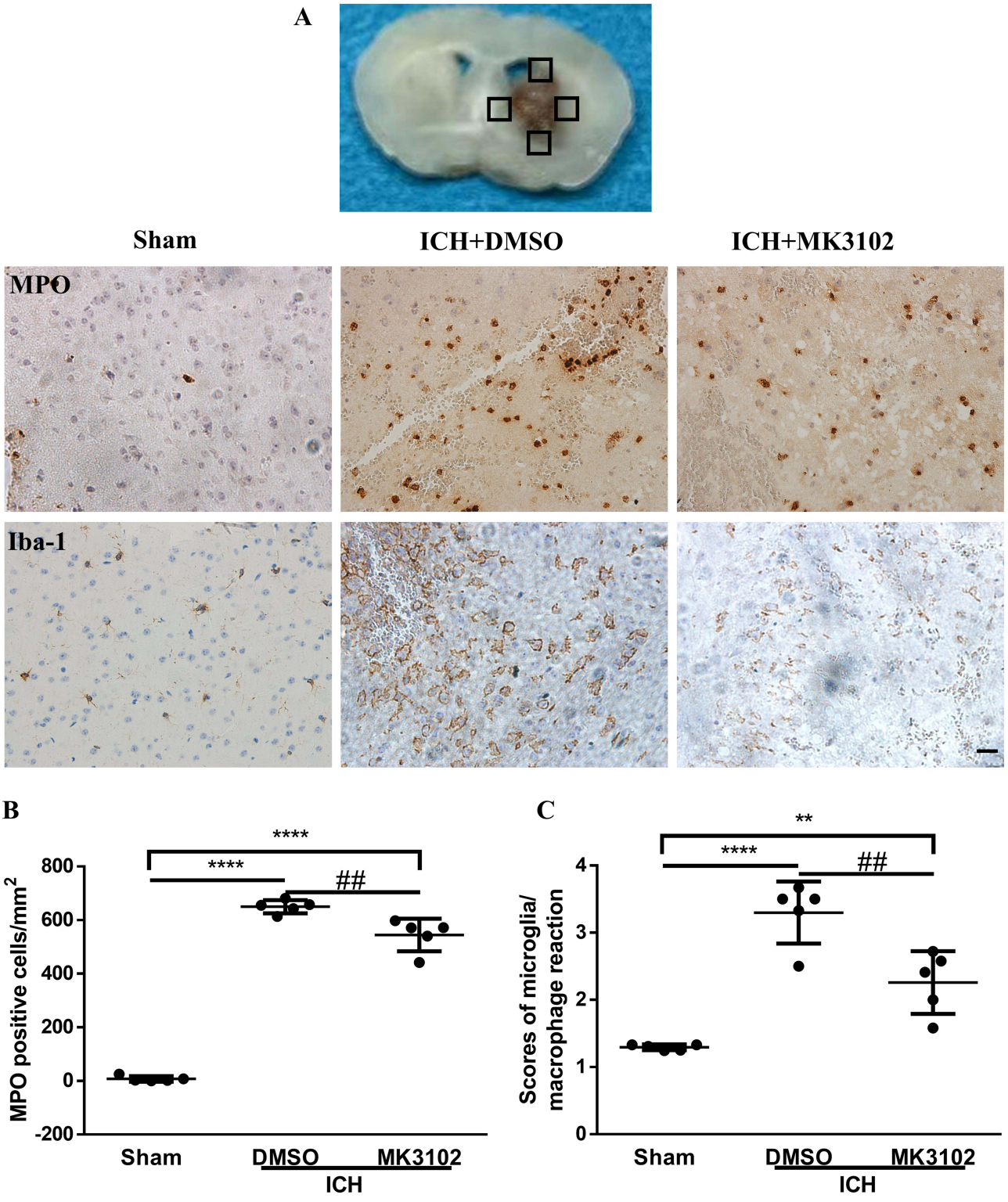

Figure 4 MK3102 alleviated the activation of microglia/macrophages and infiltration of neutrophils after ICH. (**A**) Representative images of MPO and IBA-1 in the perihematoma area at 3 days after ICH. Scale bar, 20 μm. The small black squares in the coronal section of brain indicate the area where microphotograph was taken. (**B**) Quantitative analysis of MPO positive cells. n = 5 per group. (**C**) Bar graph quantitating scores of activated microglia/macrophages after ICH. n = 5 per group. All data are displayed as mean ± SD. The difference between groups was analyzed using One-way ANOVA test. **p<0.01, ****p<0.0001 compared with sham group. ##p<0.01, compared with ICH + DMSO group.

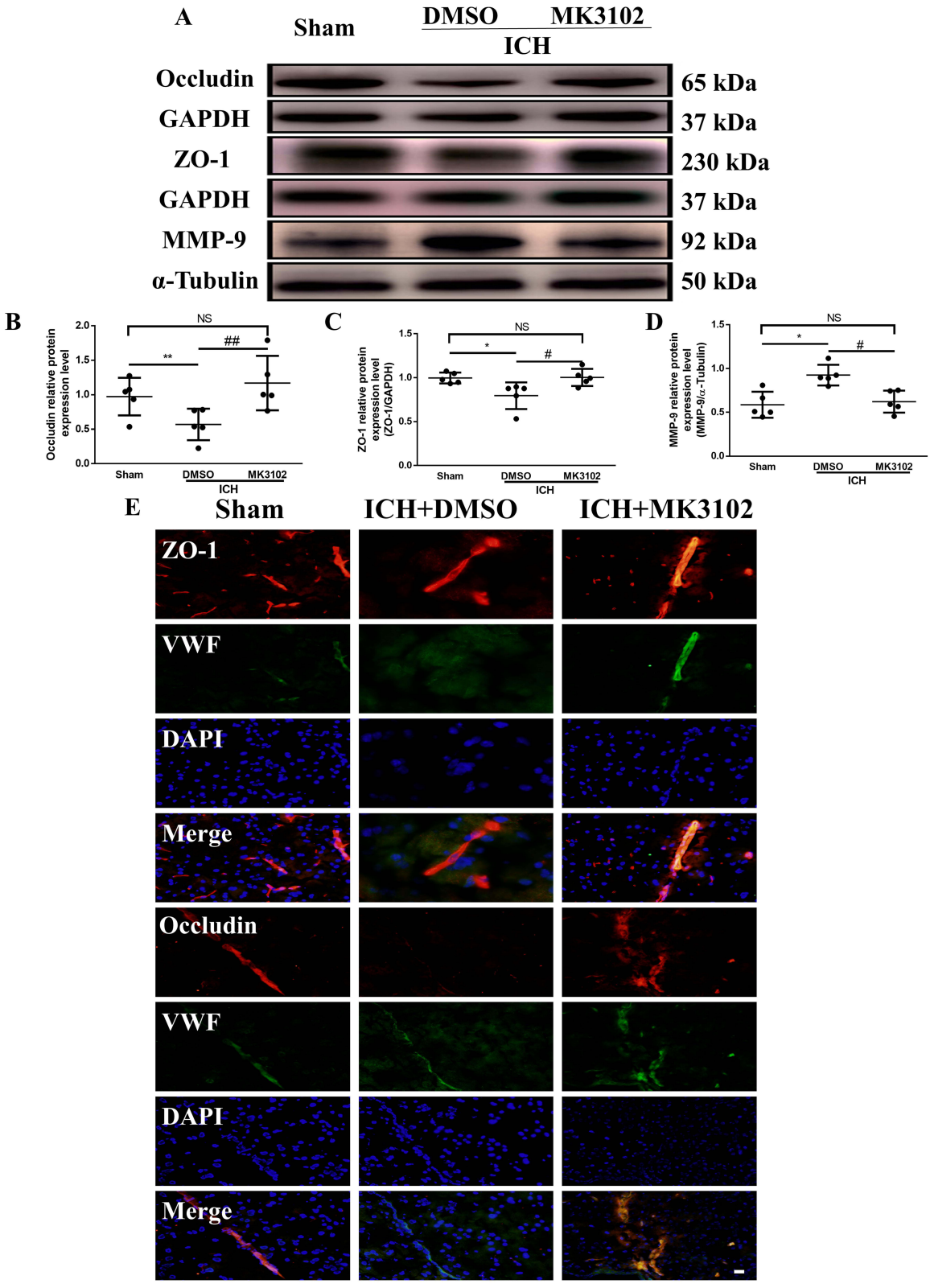

Figure 5 MK3102 prevented the change of MMP-9, ZO-1 and Occludin induced by ICH in mice. (**A**) Representative Western blot bands of MMP-9, ZO-1 and Occludin. (**B**–**D**) Quantitative analyses of relative protein expression level of MMP-9, ZO-1 and Occludin at 3 days after ICH. n = 5 per group. (**E**) Representative microphotographs of immunofluorescence co-localization staining for BBB tight junction protein ZO-1 and Occludin with vWF in the perihematomal area 3 days after ICH. Scale bar, 20 μm. All data are displayed as mean ± SD. The difference between groups was analyzed using One-way ANOVA test. *p<0.05, **p<0.01, compared with sham group. $^{\#}$p<0.05, $^{\#\#}$p<0.01, compared with the ICH + DMSO group.

Abbreviation: NS, not significant.

and Western blotting. Immunofluorescence co-localization of CX43 and GFAP (astrocyte marker) showed that CX43 was mainly expressed on astrocytes. After ICH injury, the expression of CX43 on astrocytes was increased. MK3102 treatment reversed this pathological change caused by ICH (Figure 6A). Western blot result showed that the expression level of CX43 was up-regulated after ICH injury. Compared to the ICH + DMSO group, MK3102 significantly decreased the expression level of CX43 (0.3771 ± 0.2903 versus 1.030 ± 0.1402, $p < 0.05$, Figure 6B and C).

We employed ethidium bromide staining as a surrogate of the opening of Cx43 hemichannels in this study. Ethidium bromide-positive cells were significantly increased in the ICH+DMSO group compared with the sham group (788.0 ± 114.7 versus 213.0 ± 85.34, $p < 0.0001$, Figure 6D and E), and this was lowered by MK3102 (461.6 ± 102.5 versus 788.0 ± 114.7, $p < 0.001$, Figure 6D and E) 3 days after ICH injury.

Discussion

ICH is a refractory disease with about 50% mortality rate within the first month, and more than 75% of survivors are functionally disabled at 1 year.[30] The hematoma and the toxic substances released by hematoma catabolism lead to severe inflammatory responses and oxidative stress injury, and there is irreversible BBB damage.[31,32] The disruption of BBB contributes to further infiltration of blood components, exacerbates brain edema and neurological injury after ICH. A large number of clinical studies have confirmed that brain edema caused by the destruction of the BBB is an independent predictor for worse functional outcomes in ICH patients.[33,34]

In this study, a mouse ICH model was utilized to simulate clinical ICH. Evans Blue extravasation test and brain water content measurement were used to detect the effect of DPP4 intervention on BBB after ICH. Our data show that enhanced expression of DPP4 was observed after ICH, and that DPP4 blocking with specific inhibitor MK3102 significantly lowered the expression of DPP4 and EB leakage from vessel. DPP4 inhibition also alleviated brain edema and decreased hematoma formation and neurobehavioral deficits after ICH. The protective effect of MK3102 was associated with reduced MMP-9 and CX43 levels, and preservation of the tight junction proteins ZO-1 and Occludin on endothelial cells.

DDP4 is a membrane-bound glycoprotein which is ubiquitously expressed on endothelial and epithelial cells. It exerts pleiotropic effects on glucose metabolism, inflammation, and immune system function by cleaving N-terminal dipeptides of proline or alanine-containing peptides, including incretin, neuropeptide, and chemokines.[35] For the first time, we demonstrated a significant increase in brain DPP4 expression following ICH in mice (Figure 1). It is suggested that DPP4 is involved in pathological changes after ICH. Similarly, DPP4 was upregulated in primary human brain microvascular endothelial cells after oxygen–glucose deprivation/reoxygenation stimulation.[36] DPP4 deficiency effectively protects the brain and neurological function in rodent after ICH.[37]

MK3102 is a potent DPP4 inhibitor. The expression of DPP4 was prominently reduced by MK3102 in ICH mice. Importantly, MK3102 treatment was correspondent with accelerated hematoma clearance, neuronal survival and functional recovery after ICH (Figure 2). In a model of Parkinson's disease, MK3102 attenuated motor impairment, histological aberrations and α-synuclein accumulation, and rescued dopaminergic neurons.[38] It is reasonable to speculate that the neuroprotective effect of MK3102 might be directly or indirectly related to the enhanced substrate GLP-1, GLP, neuropeptide Y, peptide YY, substance P, and stromal cell-derived factor 1. Also, the functional outcome of brain ischemia was improved by DPP-4 inhibition through the SDF-1α/CXCR4 pathway.[39]

Our previous study showed that the breakdown of the BBB (Evans Blue dye extravasation) and brain edema (observed by MRI) after ICH occurs in the ipsilateral hemisphere of the hematoma but not in the contralateral hemisphere and cerebellum.[3] In this study, we propose that DPP4 is involved in the BBB disruption induced by ICH because inhibition of DPP4 with MK3102 protects BBB integrity and reduces ipsilateral brain water content compared to the contralateral hemisphere and cerebellum (Figure 3). Consistent with our results, Du et al reported that the dysfunction of the integrity of the BBB induced by lipopolysaccharide in mice and bEnd.3 brain endothelial cells was mitigated by MK3102 administration.[18] However, the comprehensive mechanisms remain unknown, and lipopolysaccharide does not model ICH.

Microglia are the main resident immune cells in response to ICH injury. BBB permeability can be directly altered by activated microglia/macrophages via atrophy of endothelial cells, thickening of basement membranes, and degenerating pericytes.[32,40] Shortly after ICH, neutrophils infiltrate the injured brain tissue, secrete ROS and MMPs, and release neutrophil extracellular traps to further exacerbate BBB injury.[41] Previous study determined that depleting neutrophil

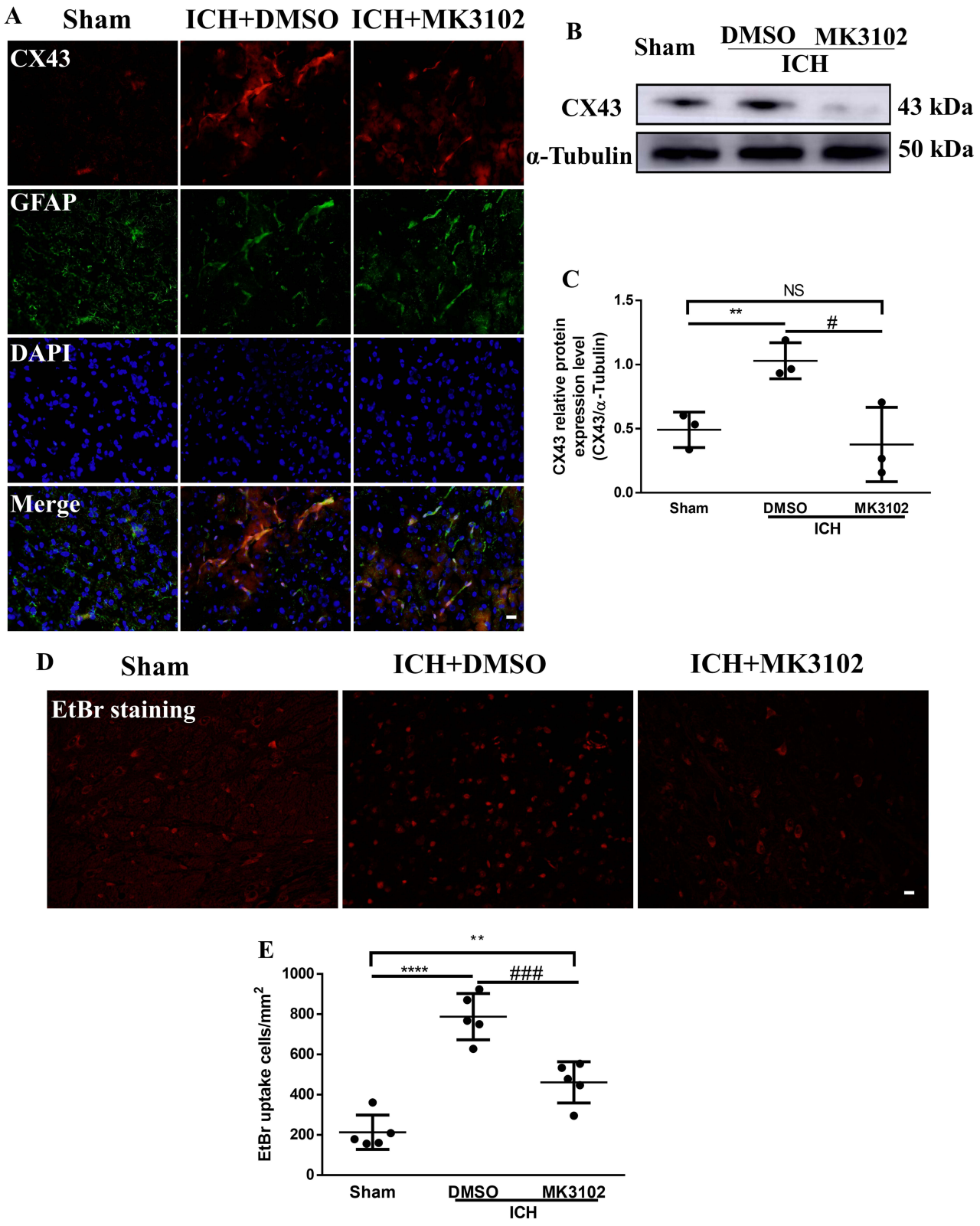

Figure 6 MK3102 inhibited the expression of CX43 on astrocytes. (**A**) Representative microphotographs of immunofluorescence co-location staining for BBB connexin junction protein CX43 with GFAP in the perihematomal area 3 days after ICH. Scale bar, 20 μm. (**B**) Representative Western blot band of CX43. (**C**) Quantitative analyses of relative protein expression level of CX43 at 3 days after ICH. n = 3 per group. (**D**) Representative microphotographs of EtBr staining in the perihematomal area. Scale bar, 20 μm. (**E**) Quantitative analysis of EtBr positive cells in the perihematomal area at 3 days after ICH. n = 5 per group. All data are displayed as mean ± SD. The difference between groups was analyzed using One-way ANOVA test. **p<0.01, ****p<0.0001, compared with sham group. #p<0.05, ###p<0.001, compared with the ICH + DMSO group.
Abbreviation: NS, not significant.

with an anti-polymorphonuclear leukocyte antibody significantly reduced MMP-9 level and BBB breakdown after ICH.[42] In this study, we examined activated microglia/macrophages and infiltrated neutrophils with immunohistochemical methods, and found that both of them were remarkably attenuated after MK3102 treatment (Figure 4). Consistent with our reports, Du et al demonstrated that MK3102 might mitigate LPS-induced neuroinflammation.[18] These results suggest that the protective effect of MK3102 on BBB integrity after ICH may be closely related to its anti-neuroinflammation.

The BBB comprises cellular constituents, including endothelial cells, pericytes, and astrocytes, as well as non-cellular components such as the cellular junctions and the basement membrane. Loss or dysfunction of any of these components can increase BBB permeability. Previous studies have shown that the BBB and junction proteins (ZO-1, occluding and cadherin-10) were markedly damaged on day 3 in collagenase-induced ICH model.[27,43] Therefore, the timepoint of 3 days after ICH was selected to test the potential protective effect of MK3102 on BBB. Our present data demonstrate that MK3102 reversed the downregulation of ZO-1 and Occludin on endothelial cells after ICH. Moreover, MMP-9, which would breach BBB integrity by degrading the basal lamina and tight junction components,[44] was reduced by MK3102 (Figure 5), which was consistent with previous report.[18] In addition, connexin 43 is distributed mainly on astrocytes[29] and the excessive opening of connexin hemichannels may increase BBB permeability by releasing toxic substances such as ATP and glutamate after ICH.[45] The expression of connexin 43 was regulated by DPP4 inhibition in the heart of diabetic mice.[46] Consistent with these results, our immunofluorescence co-localization of CX43 and GFAP showed that CX43 was mainly expressed on astrocytes. After ICH injury, the expression of CX43 and the abnormal opening of connexin 43 hemichannels on astrocytes were increased. MK3102 treatment reversed this pathological change caused by ICH (Figure 6). These data indicate that the BBB protective effect by inhibiting DPP4 with MK3102 was involved, at least in part, in MMP-9 suppression and in reducing the inflammatory response mediated by microglia/macrophages, neutrophils and connexin 43 on astrocytes.

There are several limitations in the current study. Only one treatment dose was used in this study, and further studies are needed to determine the optimal dose for the neuroprotective effects of MK3102 in ICH. Since the BBB damage in the collagenase-induced ICH model is the most severe at 3 days,[27] this study only tested the BBB protection of MK3102 at 3 days after ICH. Whether MK3102 can still reduce BBB damage and improve neurological function in other ICH model (such as autologous blood) and at a longer time point in the collagenase-induced ICH model requires further investigation. Moreover, future studies are needed to investigate the detailed molecular mechanism of BBB repair by MK3102. While MMP-9 protein level was assessed, an enzymatic assay for activity would be more reflective of the status of this metalloproteinase. In addition, only young male mice were tested in this study while increasing evidence indicates that estrogen has a neuroprotective effect in an ICH animal model;[47] therefore, the protective effect of MK3102 in aged and female animals would require investigation.

Conclusion

In summary, our findings demonstrate that DPP4 was upregulated after ICH. MK3102 effectively blocked the DPP4 increase, maintained the integrity of BBB, alleviated brain edema, and prevented functional deficits after ICH. Cellular junction proteins and MMP-9 may be implicated in the BBB protective effect of MK3102.

Data Sharing Statement

The original datasets generated for this study are included in the article, and further inquiries can be directed to the corresponding authors.

Ethics Statement

All experimental procedures were approved by the Ethics Committee of Zhengzhou University (2021326). National Standards of the People's Republic of China (GB/T 35892–2018), Laboratory Animal—Guideline for Ethical Review of Animal Welfare, was the guidance for our animal care and protocols.

Acknowledgments

The authors acknowledge operating grant support from National Key Research and Development Program of China (grant no: 2018YFC1312200), the National Natural Science Foundation of China (grants no: 82071331, 81870942, and 81520108011), and from the Canadian Institutes of Health Sciences (VWY).

Author Contributions

All authors made a significant contribution to the work reported, specifically in the conception, study design, execution, acquisition of data, analysis and interpretation. All authors took part in drafting, revising or critically reviewing the article; and they gave approval of the final version to be published. All authors have agreed on the journal to which the article has been submitted, and agree to be accountable for all aspects of the work.

Disclosure

The authors declare no potential conflicts of interest with respect to the research, authorship and/or publication of this article.

References

1. Virani SS, Alonso A, Benjamin EJ, et al. Heart disease and stroke statistics-2020 update: a report from the American heart association. *Circulation*. 2020;141:e139–e596.
2. Zhang Y, Khan S, Liu Y, Wu G, Yong V, Xue M. Oxidative stress following intracerebral hemorrhage: from molecular mechanisms to therapeutic targets. *Front Immunol*. 2022;13:847246. doi:10.3389/fimmu.2022.847246
3. Wang F, Zhang X, Liu Y, et al. Neuroprotection by ozanimod following intracerebral hemorrhage in mice. *Front Mol Neurosci*. 2022;15:927150. doi:10.3389/fnmol.2022.927150
4. Zhang X, Zhang Y, Wang F, Liu Y, Yong VW, Xue M. Necrosulfonamide alleviates acute brain injury of intracerebral hemorrhage via inhibiting inflammation and necroptosis. *Front Mol Neurosci*. 2022;15:916249.
5. Liu Y, Bai Q, Yong VW, Xue M. Emmprin promotes the expression of mmp-9 and exacerbates neurological dysfunction in a mouse model of intracerebral hemorrhage. *Neurochem Res*. 2022;47(8):2383–2395. doi:10.1007/s11064-022-03630-z
6. Sheth KN, Ropper AH. Spontaneous intracerebral hemorrhage. *N Engl J Med*. 2022;387(17):1589–1596. doi:10.1056/NEJMra2201449
7. Keep RF, Andjelkovic AV, Xiang J, et al. Brain endothelial cell junctions after cerebral hemorrhage: changes, mechanisms and therapeutic targets. *J Cereb Blood Flow Metab*. 2018;38(8):1255–1275. doi:10.1177/0271678X18774666
8. Chen S, Li L, Peng C, et al. Targeting oxidative stress and inflammatory response for blood-brain barrier protection in intracerebral hemorrhage. *Antioxid Redox Signal*. 2022;37(1–3):115–134. doi:10.1089/ars.2021.0072
9. Liu Y, Wang F, Li Z, Mu Y, Yong VW, Xue M. Neuroprotective effects of chlorogenic acid in a mouse model of intracerebral hemorrhage associated with reduced extracellular matrix metalloproteinase inducer. *Biomolecules*. 2022;12(8):1020. doi:10.3390/biom12081020
10. Li Z, Khan S, Liu Y, Wei R, Yong VW, Xue M. Therapeutic strategies for intracerebral hemorrhage. *Front Neurol*. 2022;13:1032343.
11. Zhang Y, Zhang X, Wee YV, Xue M. Vildagliptin improves neurological function by inhibiting apoptosis and ferroptosis following intracerebral hemorrhage in mice. *Neurosci Lett*. 2022;776:136579. doi:10.1016/j.neulet.2022.136579
12. Bernstein HG, Keilhoff G, Dobrowolny H, Steiner J. The many facets of cd26/dipeptidyl peptidase 4 and its inhibitors in disorders of the cns - a critical overview. *Rev Neurosci*. 2023;34(1):1–24. doi:10.1515/revneuro-2022-0026
13. Houthuijzen JM, de Bruijn R, van der Burg E, et al. Cd26-negative and cd26-positive tissue-resident fibroblasts contribute to functionally distinct caf subpopulations in breast cancer. *Nat Commun*. 2023;14(1):183. doi:10.1038/s41467-023-35793-w
14. Shao Z, Li X, Xu X, Chen P. DPP-4 inhibitor linagliptin ameliorates imiquimod-induced psoriasis-like skin alterations in type 2 diabetic mice by inhibiting the MAPK/NF-kappaB inflammatory pathway. *Drug Dev Res*. 2022;83:1373–1382. doi:10.1002/ddr.21966
15. Nimlamool W, Andrews RM, Falk MM. Connexin43 phosphorylation by PKC and MAPK signals VEGF-mediated gap junction internalization. *Mol Biol Cell*. 2015;26:2755–2768. doi:10.1091/mbc.E14-06-1105
16. Fan SH, Xiong QF, Wang L, Zhang LH, Shi YW. Glucagon-like peptide 1 treatment reverses vascular remodelling by downregulating matrix metalloproteinase 1 expression through inhibition of the erk1/2/nf-kappab signalling pathway. *Mol Cell Endocrinol*. 2020;518:111005. doi:10.1016/j.mce.2020.111005
17. Biftu T, Sinha-Roy R, Chen P, et al. Omarigliptin (mk-3102): a novel long-acting dpp-4 inhibitor for once-weekly treatment of type 2 diabetes. *J Med Chem*. 2014;57:3205–3212. doi:10.1021/jm401992e
18. Du H, Wang S. Omarigliptin mitigates lipopolysaccharide-induced neuroinflammation and dysfunction of the integrity of the blood-brain barrier. *ACS Chem Neurosci*. 2020;11:4262–4269. doi:10.1021/acschemneuro.0c00537
19. Xue M, Del BM. Intracerebral injection of autologous whole blood in rats: time course of inflammation and cell death. *Neurosci Lett*. 2000;283:230–232. doi:10.1016/S0304-3940(00)00971-X
20. Festing MFW, Altm DG. Guidelines for the design and statistical analysis of experiments using laboratory animals. *ILAR J*. 2002;43:244–258. doi:10.1093/ilar.43.4.244
21. Ayoub BM, Mowaka S, Safar MM, et al. Repositioning of omarigliptin as a once-weekly intranasal anti-parkinsonian agent. *Sci Rep*. 2018;8:8959. doi:10.1038/s41598-018-27395-0
22. Liu Y, Li Z, Khan S, et al. Neuroprotection of minocycline by inhibition of extracellular matrix metalloproteinase inducer expression following intracerebral hemorrhage in mice. *Neurosci Lett*. 2021;764:136297. doi:10.1016/j.neulet.2021.136297
23. Li Z, Liu Y, Wei R, Khan S, Xue M, Yong VW. The combination of deferoxamine and minocycline strengthens neuroprotective effect on acute intracerebral hemorrhage in rats. *Neurol Res*. 2021;43(10):854–864. doi:10.1080/01616412.2021.1939487
24. Wu D, Lai N, Deng R, et al. Activated wnk3 induced by intracerebral hemorrhage deteriorates brain injury maybe via wnk3/spak/nkcc1 pathway. *Exp Neurol*. 2020;332:113386. doi:10.1016/j.expneurol.2020.113386
25. Xie RX, Li DW, Liu XC, et al. Carnosine attenuates brain oxidative stress and apoptosis after intracerebral hemorrhage in rats. *Neurochem Res*. 2017;42:541–551. doi:10.1007/s11064-016-2104-9
26. Ma Q, Huang B, Khatibi N, et al. Pdgfr-alpha inhibition preserves blood-brain barrier after intracerebral hemorrhage. *Ann Neurol*. 2011;70:920–931. doi:10.1002/ana.22549

27. Jia P, He J, Li Z, et al. Profiling of blood-brain barrier disruption in mouse intracerebral hemorrhage models: collagenase injection vs. autologous arterial whole blood infusion. *Front Cell Neurosci*. 2021;15:699736. doi:10.3389/fncel.2021.699736
28. Xue M, Mikliaeva EI, Casha S, Zygun D, Demchuk A, Yong VW. Improving outcomes of neuroprotection by minocycline: guides from cell culture and intracerebral hemorrhage in mice. *Am J Pathol*. 2010;176:1193–1202. doi:10.2353/ajpath.2010.090361
29. Yu H, Cao X, Li W, et al. Targeting connexin 43 provides anti-inflammatory effects after intracerebral hemorrhage injury by regulating yap signaling. *J Neuroinflammation*. 2020;17(1):322. doi:10.1186/s12974-020-01978-z
30. Magid J, Girard R, Polster S, et al. Cerebral hemorrhage: pathophysiology, treatment, and future directions. *Circ Res*. 2022;130(8):1204–1229. doi:10.1161/CIRCRESAHA.121.319949
31. Zhang Y, Khan S, Liu Y, et al. Modes of brain cell death following intracerebral hemorrhage. *Front Cell Neurosci*. 2022;16:799753. doi:10.3389/fncel.2022.799753
32. Bai Q, Xue M, Yong VW. Microglia and macrophage phenotypes in intracerebral haemorrhage injury: therapeutic opportunities. *Brain*. 2020;143(5):1297–1314. doi:10.1093/brain/awz393
33. Urday S, Beslow LA, Dai F, et al. Rate of perihematomal edema expansion predicts outcome after intracerebral hemorrhage. *Crit Care Med*. 2016;44:790–797. doi:10.1097/CCM.0000000000001553
34. Murthy SB, Moradiya Y, Dawson J, Lees KR, Hanley DF, Ziai WC. Perihematomal edema and functional outcomes in intracerebral hemorrhage: influence of hematoma volume and location. *Stroke*. 2015;46(11):3088–3092. doi:10.1161/STROKEAHA.115.010054
35. Ghersi G, Zhao Q, Salamone M, Yeh Y, Zucker S, Chen WT. The protease complex consisting of dipeptidyl peptidase iv and seprase plays a role in the migration and invasion of human endothelial cells in collagenous matrices. *Cancer Res*. 2006;66:4652–4661. doi:10.1158/0008-5472.CAN-05-1245
36. Zeng X, Li X, Chen Z, Yao Q. Dpp-4 inhibitor saxagliptin ameliorates oxygen deprivation/reoxygenation-induced brain endothelial injury. *Am J Transl Res*. 2019;11:6316–6325.
37. Yip HK, Lee MS, Li YC, et al. Dipeptidyl peptidase-4 deficiency effectively protects the brain and neurological function in rodent after acute hemorrhagic stroke. *Int J Biol Sci*. 2020;16(16):3116–3132. doi:10.7150/ijbs.42677
38. Michel HE, Tadros MM, Hendy MS, Mowaka S, Ayoub BM. Omarigliptin attenuates rotenone-induced Parkinson's disease in rats: possible role of oxidative stress, endoplasmic reticulum stress and immune modulation. *Food Chem Toxicol*. 2022;164:113015.
39. Chiazza F, Tammen H, Pintana H, et al. The effect of dpp-4 inhibition to improve functional outcome after stroke is mediated by the sdf-1alpha/cxcr4 pathway. *Cardiovasc Diabetol*. 2018;17(1):60. doi:10.1186/s12933-018-0702-3
40. Nadeau CA, Dietrich K, Wilkinson CM, et al. Prolonged blood-brain barrier injury occurs after experimental intracerebral hemorrhage and is not acutely associated with additional bleeding. *Transl Stroke Res*. 2019;10:287–297. doi:10.1007/s12975-018-0636-9
41. Xue M, Yong VW. Neuroinflammation in intracerebral haemorrhage: immunotherapies with potential for translation. *Lancet Neurol*. 2020;19(12):1023–1032. doi:10.1016/S1474-4422(20)30364-1
42. Moxon-Emre I, Schlichter LC. Neutrophil depletion reduces blood-brain barrier breakdown, axon injury, and inflammation after intracerebral hemorrhage. *J Neuropathol Exp Neurol*. 2011;70(3):218–235. doi:10.1097/NEN.0b013e31820d94a5
43. Wang T, Chen X, Wang Z, et al. Poloxamer-188 can attenuate blood-brain barrier damage to exert neuroprotective effect in mice intracerebral hemorrhage model. *J Mol Neurosci*. 2015;55:240–250. doi:10.1007/s12031-014-0313-8
44. Li H, Sheng Z, Khan S, et al. Matrix metalloproteinase-9 as an important contributor to the pathophysiology of depression. *Front Neurol*. 2022;13:861843. doi:10.3389/fneur.2022.861843
45. Zhang Y, Khan S, Liu Y, et al. Gap junctions and hemichannels composed of connexins and pannexins mediate the secondary brain injury following intracerebral hemorrhage. *Biology*. 2022;11:27. doi:10.3390/biology11010027
46. Li X, Meng C, Han F, et al. Vildagliptin attenuates myocardial dysfunction and restores autophagy via mir-21/spry1/erk in diabetic mice heart. *Front Pharmacol*. 2021;12:634365. doi:10.3389/fphar.2021.634365
47. Zheng Y, Hu Q, Manaenko A, et al. 17β-estradiol attenuates hematoma expansion through estrogen receptor α/silent information regulator 1/nuclear factor-kappa b pathway in hyperglycemic intracerebral hemorrhage mice. *Stroke*. 2015;46(2):485–491. doi:10.1161/STROKEAHA.114.006372